ORIGINAL ARTICLE

Journal of Cachexia, Sarcopenia and Muscle 2019; **10**: 894–902
Published online 15 May 2019 in Wiley Online Library (wileyonlinelibrary.com) **DOI:** 10.1002/jcsm.12430

Psoas muscle fluorine-18-labelled fluoro-2-deoxy-d-glucose uptake associated with the incidence of existing and incipient metabolic derangement

Ji Young Kim[1], Dae Won Jun[2]*, Jun Choi[3], Eunwoo Nam[4], Donghee Son[4] & Yun Young Choi[1]

[1]*Department of Nuclear Medicine, Hanyang University School of Medicine, Seoul, South Korea,* [2]*Department of Internal Medicine, Hanyang University School of Medicine, Seoul, South Korea,* [3]*Department of Fusion Data Analytics, School of Industrial Management Engineering, Korea University, Seoul, South Korea,* [4]*Biostatistical Consulting and Research Lab, Hanyang University School of Medicine, Seoul, South Korea*

Abstract

Background Skeletal muscle glucose utilization is an important component of whole-body glucose consumption in normal humans. Fluorine-18-labelled fluoro-2-deoxy-d-glucose (^{18}F-FDG) is a non-invasive molecular imaging probe for evaluating tissue glucose utilization. It remains unclear whether or not ^{18}F-FDG uptake by skeletal muscle has utility as a biomarker for metabolic derangement. We investigated the utility of measurement of muscle ^{18}F-FDG positron emission tomography/computed tomography uptake as a surrogate marker for existing and incipient metabolic abnormalities.

Methods Fluorine-18-labelled fluoro-2-deoxy-d-glucose (^{18}F-FDG) uptakes of insulin-sensitive organs (liver, pancreas, mesenteric visceral fat, psoas muscle, and abdominal subcutaneous fat) and their association with metabolic abnormalities were evaluated in an experimental group comprising 91 men and 66 women (mean age 49.9 ± 11.1 years). In this cross-sectional cohort, we assessed the predictive power of the optimal cut-off ^{18}F-FDG uptake [maximum standardized uptake value (SUV_{max})]. We confirmed its feasibility and reliability for diagnosis of existing and incipient metabolic derangement in the validation group (longitudinal cohort comprising 91 men and 67 women; mean age 52.6 ± 7.9 years).

Results Fluorine-18-labelled fluoro-2-deoxy-d-glucose (^{18}F-FDG) uptake (SUV_{max}) of psoas muscle was strongly correlated with clinical metabolic parameters in the experimental group. It was positively correlated with waist circumference, body mass index, fasting glucose, triglyceride, systolic and diastolic pressure, and negatively correlated with high-density lipoprotein cholesterol levels (for all, $P < 0.05$). SUV_{max} of the psoas muscle also showed the best area under the curve value (0.779) as a predictor of metabolic syndrome (MetS) in the experimental group. Using the optimal cut-off SUV_{max} of 1.34, the sensitivity, specificity, accuracy, positive, and negative predictive value for predicting existing MetS in the experimental group were 70.0%, 84.6%, 80.9%, 60.9%, and 89.2%, respectively. In the validation group, corresponding values were 47.6%, 92.3%, 86.1%, 50.0%, and 91.6%, respectively. Existing and incipient MetS were significantly higher in subjects with high ^{18}F-FDG uptake by the psoas muscle ($SUV_{max} > 1.34$). Subjects with higher psoas muscle SUV_{max} had a 3.3-fold increased risk of developing MetS ($P = 0.017$).

Conclusions Fluorine-18-labelled fluoro-2-deoxy-d-glucose (^{18}F-FDG) uptake of psoas muscle is a promising surrogate marker for existing and incipient metabolic derangement.

Keywords ^{18}F-FDG; Standardized uptake value; Psoas muscle; Metabolic syndrome; Surrogate marker

Received: 11 May 2018; Accepted: 1 March 2019
**Correspondence to: Dae Won Jun, MD, PhD, Department of Internal Medicine, Hanyang University College of Medicine, 222-1 Wangsimni-ro, Seongdong-gu, Seoul 04763, South Korea. Tel: +82 2 2290 8338; Fax: +82 2 972 0068, Email: noshin@hanyang.ac.kr*

Introduction

The increasing prevalence of metabolic diseases with advancing age is a major public health concern worldwide. It is well known that both skeletal muscle volume[1,2] and quality are key determinants of the risk of metabolic abnormalities.[1] Skeletal muscle glucose utilization (SMGU) accounts for 70–80% of whole-body glucose consumption in normal humans and is thought to be the most important determinant of whole-body insulin resistance (IR).[3]

Fluorine-18-labelled fluoro-2-deoxy-d-glucose (^{18}F-FDG), a glucose analog, is a non-invasive molecular imaging probe that is used for quantitative *in vivo* evaluation of glucose utilization in tissues and whole organs. ^{18}F-FDG positron emission tomography/computed tomography (PET/CT) has been used widely for evaluation of neoplastic diseases[4–7] and less commonly for non-neoplastic inflammatory diseases,[7,8] as well as for risk stratification in patients with carotid atherosclerosis.[9–12]

The utility of ^{18}F-FDG uptake as a biomarker for metabolic derangement is unclear. Previous reports using this probe provided valuable insights into IR, and it has been used to measure SMGU *in vivo*.[3,13–16] The rate of glucose disposal during the hyperinsulinemic euglycemic clamp test was correlated with SMGU estimated by dynamic or static ^{18}F-FDG PET.[3,13–16] However, previous studies had small sample sizes and were experimental; therefore, clinical assessments are needed.

We investigated the biodistribution of ^{18}F-FDG in insulin-sensitive organs, including the liver, skeletal muscle, and fat tissue, to relate this marker to metabolic derangement in an average-risk population. We also aimed to validate ^{18}F-FDG uptake of insulin-sensitive organs as a surrogate marker to predict MetS.

Research design and methods

Study design

In a single centre, we retrospectively reviewed the records of ^{18}F-FDG PET/CT assessments that were included in routine wellness check-ups. The dataset comprised an experimental and a validation group.

Between January and December 2014, 196 subjects underwent ^{18}F-FDG PET/CT. Thirty-nine were excluded for one or more of the following reasons: positive serologic markers for hepatitis B virus surface antigen or hepatitis C antibody, a history of taking herbal medicines, steroids, or amiodarone (all of which are known to cause fatty liver) in the previous month, and suspicion of a malignant tumour on abdominal ultrasonography. Subjects who received anti-diabetic drugs, cholesterol-lowering agents, and anti-hypertensive drugs were included in the study. Finally, 157 subjects (91 men and 66 women; mean age 49.9 ± 11.1 years) constituted the experimental group (cross-sectional cohort).

We retrospectively reviewed subjects who had one or more follow-up health checks after ^{18}F-FDG PET/CT scans, between January 2009 and December 2012. The exclusion criteria were same as those in the experimental group, yielding a total of 158 subjects (91 men and 67 women; mean age 52.6 ± 7.9 years) with complete records of the required clinical parameters. These subjects comprised the validation group (longitudinal cohort) (Table 1).

The study protocol was reviewed and approved by the institutional review board at our institution (approval number HYIRB 2015-10-006-001).

Table 1 Baseline characteristics of the experimental and validation groups

	Experimental group (n = 157)	Validation group (n = 158)
Age (years)	49.90 ± 11.11	52.58 ± 7.85
Male sex (%)	91 (57.96)	91 (57.59)
Waist (cm)	91.73 ± 14.22	89.58 ± 12.33
BMI (kg/m^2)	26.88 ± 5.18	25.10 ± 3.92
Triglyceride (mg/dL)	94 (66–144)	103 (75–147)
LDL cholesterol (mg/dL)	131.49 ± 36.91	123.46 ± 33.99
Total cholesterol (mg/dL)	208.20 ± 41.38	206.09 ± 37.61
HDL cholesterol (mg/dL)	49.83 ± 13.56	52.30 ± 12.30
Systolic pressure (mmHg)	129.43 ± 20.02	120.99 ± 16.73
Diastolic pressure (mmHg)	77.80 ± 13.47	75.04 ± 11.94
Fasting glucose (mg/dL)	90 (81–98)	89 (82–102)
AST (U/L)	22 (18–27)	22 (18–29)
ALT (U/L)	25 (18–37)	21 (16–34)
Bilirubin (mg/dL)	0.77 (0.56–1.04)	0.70 (0.51–1.00)
GGT (U/L)	24 (17–43)	25 (16–40)
MetS (%)	40 (25.48)	25 (15.82)

Numerical quantitative data were presented by 'mean ± SD' or 'median ($Q_1 - Q_3$)' and tested by a t-test or a Mann–Whitney U test, and categorical data were presented by 'frequency (%)' and tested by a chi-squared test. ALT, alanine aminotransferase; AST, aspartate aminotransferase; BMI, body mass index; GGT: γ-glutamyl transferase; HDL, high-density lipoprotein; LDL, low-density lipoprotein; MetS, metabolic syndrome

DOI: 10.1002/jcsm.12430

Definitions

The diagnostic criteria for metabolic syndrome (MetS) according to the National Cholesterol Education Program Adult Treatment Panel III[17] are based on specific cut-off points in any three or more of the following five risk determinants: (i) abdominal obesity, waist circumference >90 (Eastern subjects) or 102 cm (Western subjects) in men and >80 (Eastern subjects) or 88 cm (Western subjects) in women; (ii) fasting triglyceride concentrations ≥150 mg/dL or specific treatment for this lipid abnormality (dyslipidemia); (iii) fasting high-density lipoprotein (HDL) cholesterol <40 mg/dL in men and <50 mg/dL in women or specific treatment for this lipid abnormality (dyslipidemia); (iv) BP ≥ 130/ ≥ 85 mmHg (either value) or treatment for previously diagnosed hypertension; and (v) fasting blood glucose ≥110 mg/dL or a previous diabetes diagnosis. Incipient MetS was defined as the new onset of any three or more of the above five determinants during follow-up period in validation group detected by reviews of hospital charts and laboratory results.[17]

Biochemical analyses

After an overnight fast, peripheral blood was drawn from an antecubital vein to measure fasting blood glucose (mg/dL), triglyceride (mg/dL), total cholesterol, low-density lipoprotein (mg/dL), HDL (mg/dL) cholesterol, aspartate aminotransferase (U/L), alanine aminotransferase (U/L), bilirubin (mg/dL), and γ-glutamyl transferase (U/L).

Fluorine-18-labelled fluoro-2-deoxy-d-glucose positron emission tomography/computed tomography imaging and analysis

Fluorine-18-labelled fluoro-2-deoxy-d-glucose (^{18}F-FDG) PET/CT was performed with a dedicated PET/CT scanner (Biograph 6; Siemens Medical Systems, Knoxville, TN). All subjects fasted for >6 h before ^{18}F-FDG administration. Approximately 60 min after intravenous injection of ^{18}F-FDG (5.18 MBq/kg; mean, 565 MBq; range, 333–962 MBq), CT images were acquired, immediately followed by whole-body PET images from the base of the skull to the upper thigh. The acquisition time for PET was 2.0 or 3.0 min per table position. The image reconstruction matrix was 168 × 168 with a transverse field of view of 50 cm. The images were reconstructed using a standard iterative algorithm (OSEM) and analysed at a dedicated workstation equipped with fusion software capable of displaying CT, PET, and PET/CT images (MMWP, Siemens Medical Systems, Hoffman Estate, IL, USA). A dual board-certified physician in radiology and nuclear medicine reviewed all images. To evaluate metabolism of the liver, pancreas, mesenteric visceral fat, psoas muscle, and abdominal subcutaneous fat, several fixed or flexible spherical volumes of interest (VOIs) were used to calculate the standardized uptake value (SUV) according to the following equation: SUV = [regional activity (mCi/mL)]/[injected dose (mCi)/body weight (g)]. For the liver, two fixed VOIs 6 cm in diameter (volume, 113.06 cm^3) were manually drawn over the anterosuperior and posteroinferior portions of the right lobe of the liver, carefully avoiding the central vascular area. These two values were averaged to estimate the mean SUV (SUV_{mean}) of the liver. For the psoas muscle and subcutaneous fat, two fixed VOIs 3 cm in diameter (volume, 14.13 cm^3) were manually drawn over the right psoas muscle and subcutaneous layer of the right gluteal area to assess the maximum SUV (SUV_{max}) of each VOI. For the pancreas and mesenteric visceral fat, two small and flexible VOIs were drawn over the pancreas tail and retroperitoneal area around the right kidney, avoiding small vessel activity, to assess the SUV_{max} of each VOI.

Statistical analyses

Continuous data are presented as means ± SD or medians (Q_1–Q_3) and compared between groups using either Student's *t*-tests or Mann–Whitney *U* tests as appropriate, following normality tests. Categorical data are presented as frequencies (%) and compared using chi-squared tests. In the experimental group, correlation analysis using Spearman rank correlation coefficients and simple and multiple logistic regression analyses were used to identify independent predictors of MetS.

The areas under the receiver operating characteristic (AUROC) curves were estimated to assess discriminative ability, and AUROC based on psoas muscle was compared with other potential predictors using pairwise Z-tests with Bonferroni corrections. The known cut-off values were adopted for given clinical predictors, whereas optimal cut-off values were determined for PET/CT predictors to maximize the value of the Youden index for the receiver operating characteristic curve. The sensitivity, specificity, accuracy, and positive and negative predictive values (PPV and NPV) were calculated and compared between the psoas muscle and other predictors using post hoc comparisons with Bonferroni correction after Cochran's Q or chi-squared tests.

Finally, new-onset event-free MetS survivors and subjects with other metabolic derangements indicated by optimal cut-off values of SUV_{max} in the psoas muscle group were assessed using Kaplan–Meier survival analysis and compared using the log-rank test. Also, multiple Cox's proportional hazard regression analyses were performed for the psoas muscle groups to assess the independent predictors of the presence or absence of these new-onset events. *P*-values <0.05 were considered statistically significant. All statistical analyses were performed using SAS 9.4 (SAS Institute Inc.,

Cary, NC, USA), SPSS version 23 (IBM Corp., Armonk, NY, USA), and MedCalc Version 18.10.2 (Medcalc Software bvba, Ostend, Belgium).

Results

Correlation between fluorodeoxyglucose uptake of various organs and metabolic parameters

Fluorine-18-labelled fluoro-2-deoxy-d-glucose (^{18}F-FDG) uptakes in psoas muscle, mesenteric visceral fat, abdominal subcutaneous fat, pancreas, and liver were all positively correlated with waist circumference, body mass index (BMI), systolic and diastolic pressures, and fasting glucose (this last with the exception of pancreas) (Table 2). Among these, ^{18}F-FDG uptake (SUV_{max}) of psoas muscle showed the strongest correlation with these clinical metabolic parameters in the experimental group.

Fluorodeoxyglucose uptake of psoas muscle as an independent risk factor for metabolic syndrome

Simple and multiple logistic regression analyses identified SUV_{max} of the psoas muscle in the experimental group as an independent risk factor for MetS [adjusted odds ratio (OR) 49.21; 95% confidence interval 1.12–999.99; $P = 0.044$] after adjusting for age, waist circumference, BMI, triglycerides, HDL cholesterol, systolic and diastolic pressure, and fasting glucose (Table 3).

Assessment of areas under the receiver operating characteristic and cut-off value of maximum standardized uptake value for psoas muscle and predictive performance for metabolic syndrome in the experimental group

The SUV_{max} of the psoas muscle had the highest AUROC value, identifying it as a significant predictor of existing MetS (0.779,

Table 2 Spearman rank correlation coefficients between metabolic parameters and FDG uptake in various organs in the experimental group

	Liver	Pancreas	Visceral fat	SubQ fat	Psoas muscle
Waist (cm)	0.42*	0.38*	0.44*	0.41*	0.72*
BMI (kg/m^2)	0.38*	0.40*	0.49*	0.44*	0.74*
Triglyceride (mg/dL)	0.29*	0.08	0.06	0.15	0.26*
LDL cholesterol (mg/dL)	0.02	−0.07	−0.30*	−0.32*	0.05
Total cholesterol (mg/dL)	0.07	−0.13	−0.32*	−0.28*	0.03
HDL cholesterol (mg/dL)	−0.12	−0.27*	−0.13	−0.14	−0.22*
Systolic pressure (mmHg)	0.22*	0.20*	0.27*	0.26*	0.43*
Diastolic pressure (mmHg)	0.18*	0.17*	0.21*	0.18*	0.32*
Fasting glucose (mg/dL)	0.24*	0.13	0.21*	0.28*	0.30*

BMI, body mass index; FDG, fluorodeoxyglucose; HDL, high-density lipoprotein; LDL, low-density lipoprotein; SubQ, subcutaneous.
*Correlation coefficients are significantly different from 0 ($P < 0.05$).

Table 3 Identification of risk factors of metabolic syndrome in the experimental group

	Univariate logistic regression			Multivariate logistic regression[a]		
Variables	Unadjusted OR	95% CI	*P*-value	Adjusted OR	95% CI	*P*-value
Age	1.04	1.00–1.07	0.0429*	1.15	1.04–1.29	0.0102*
Sex	0.78	0.37–1.62	0.5011			
Waist	1.10	1.06–1.14	<0.0001*	0.83	0.70–0.99	0.0425*
BMI	1.31	1.19–1.44	<0.0001*	1.98	1.19–3.32	0.0091*
Triglycerides	1.03	1.02–1.04	<0.0001*	1.07	1.03–1.10	<0.0001*
LDL cholesterol	1.00	0.99–1.01	0.4107			
Total cholesterol	1.00	0.99–1.01	0.8885			
HDL cholesterol	0.93	0.89–0.96	0.0001*	0.99	0.93–1.05	0.7474
Systolic pressure	1.05	1.03–1.07	<0.0001*	0.98	0.90–1.07	0.6584
Diastolic pressure	1.05	1.02–1.08	0.0004*	1.07	0.95–1.22	0.2594
Fasting glucose	1.07	1.04–1.10	<0.0001*	1.04	1.00–1.09	0.0331*
Psoas muscle	19.61	5.92–64.95	<0.0001*	49.21	1.116–999.999	0.0437*

BMI, body mass index; CI: confidence interval; HDL, high-density lipoprotein; LDL, low-density lipoprotein; OR, odds ratio.
*Unadjusted and adjusted OR are significantly different from 1 ($P < 0.05$).
[a]The multivariate logistic regression model incorporates possible risk factors which are significant in univariate logistic regression analysis such as age, waist, BMI, triglycerides, HDL cholesterol, systolic blood pressure, diastolic blood pressure, fasting glucose, and fluorodeoxyglucose uptake of the psoas muscle.

DOI: 10.1002/jcsm.12430

cut-off at 1.34) relative to fluorodeoxyglucose uptake of other insulin-sensitive organs: SUV_{mean} of liver (0.707, cut-off at 2.34), SUV_{max} values for pancreas (0.625, cut-off at 2.11), visceral mesenteric fat (0.696, cut-off at 0.58), and abdominal subcutaneous fat (0.740, cut-off at 0.39) (Figure 1A). As a predictor of MetS, SUV_{max} of the psoas muscle (0.779, cut-off at 1.34) was comparable to the AUROCs among other clinical predictors. There were no significant differences among metabolic risk factors: BMI (0.837, cut-off at 25 kg/m2), triglyceride (0.904, cut-off at 150 mg/dL), HDL cholesterol (0.755, cut-off at 40 mg/dL in men and at 50 mg/dL in women), systolic pressure (0.742, cut-off at 130 mmHg), and fasting glucose (0.839, cut-off at 110 mg/dL) (Figure 1B).

In the experimental group, when the cut-off SUV_{max} for psoas muscle was set at 1.34, the sensitivity, specificity, accuracy, PPV, and NPV for predicting MetS were 70.0%, 84.6%, 80.9%, 60.9%, and 89.2%, respectively. Relative to the diagnostic values of clinical predictors (BMI, triglyceride, HDL cholesterol, systolic pressure, diastolic pressure, and fasting glucose), the specificity and accuracy of psoas muscle metabolism in the prediction of MetS was significantly higher than those of BMI and systolic pressure (Table 4).

Assessment of predictive performance for metabolic syndrome in validation group

We applied this cut-off (1.34) SUV_{max} for psoas muscle in the validation group to confirm its feasibility and reliability. The AUROC value for prediction of MetS was 0.709, and the sensitivity, specificity, accuracy, PPV, and NPV for predicting MetS were 47.6%, 92.3%, 86.1%, 50.0%, and 91.6%, respectively. Again, relative to the diagnostic values of clinical predictors (BMI, triglyceride, HDL cholesterol, systolic pressure, diastolic pressure, and fasting glucose), the specificity of psoas muscle metabolism as a predictor of MetS was higher than those of BMI, systolic pressure, and fasting glucose; its accuracy was higher than that of BMI (Table 5).

In subjects with $SUV_{max} > 1.34$ in the psoas muscle, the prevalence rates for metabolic abnormalities were significantly higher than those in subjects with $SUV_{max} \leq 1.34$ in the psoas muscle in both the experimental group (Table S1) and the validation group (Table S2).

Survival analysis for incipient metabolic syndrome and its determinants in the validation group

The median duration of follow-up in the validation cohort was 2.25 years. The Kaplan–Meier curve showed that the cumulative incidence of new onset MetS (Figure 2A) and other clinical risk parameters for MetS (Figure 2B) was significantly higher in subjects with higher psoas muscle uptakes of ^{18}F-FDG ($SUV_{max} > 1.34$) than in those with lower values ($SUV_{max} \leq 1.34$) (log-rank test for MetS, $P = 0.0093$; HDL-cholesterolemia, $P < 0.0001$; hypertension, $P = 0.0001$; hyperglycaemia, $P = 0.0458$). In a Cox proportional hazards model adjusted for age and sex, ^{18}F-FDG uptake (SUV_{max}) in the psoas muscle was associated with increased risks of incipient MetS [hazard ratio (HR) 3.26, $P = 0.0174$], low HDL

Figure 1 Comparisons of receiver operating characteristic (ROC) curves and the areas under the receiver operating characteristic (AUROC) among (A) Fluorodeoxyglucose uptake of insulin sensitive organs on fluorine-18-labeled fluoro-2-deoxy-d-glucose positron emission tomography/computed tomography and (B) other clinical predictors and fluorodeoxyglucose uptake of psoas muscle for the discrimination of metabolic syndrome (MetS) in experimental group. *Significant difference by pairwise Z-test with Bonferroni correction with respect to psoas muscle ($P < 0.05$). †Cut-off value is determined to maximize the value of Youden index for ROC curve using Medcalc. BMI, body mass index; HDL, high-density lipoprotein; SubQ, subcutaneous; TG, triglyceride.

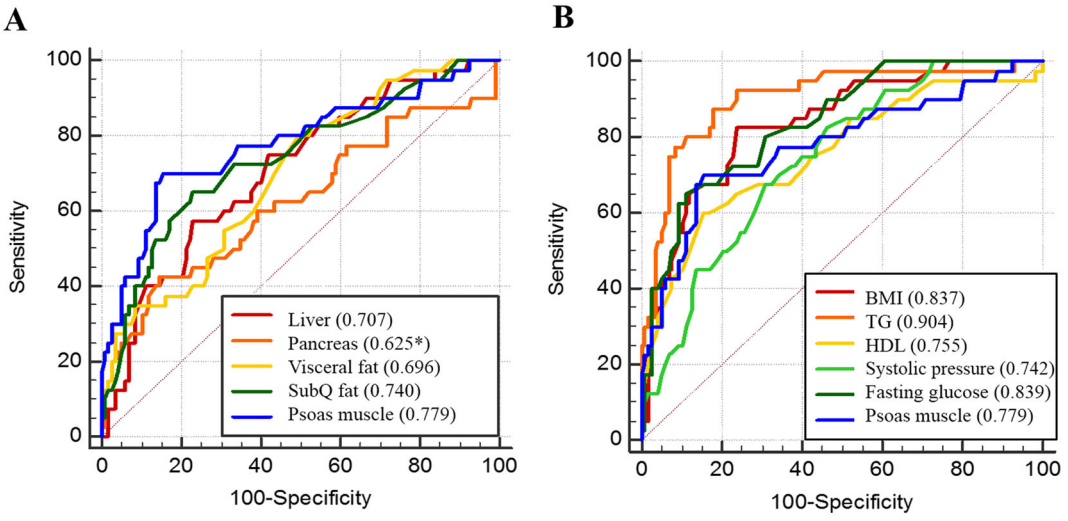

DOI: 10.1002/jcsm.12430

Table 4 Predictive performance of clinical and other predictors in the experimental group for metabolic syndrome for metabolic syndrome

	Variable	Sensitivity[a]	Specificity[a]	Accuracy[a]	PPV[b]	NPV[b]
PET/CT predictor[c]	Liver (>2.34)	57.50 (23/40)	76.92 (90/117)	71.97 (113/157)	46.00 (23/50)	84.11 (90/107)
	Pancreas (>2.11)	42.50* (17/40)	85.47 (100/117)	74.52 (117/157)	50.00 (17/34)	81.30 (100/123)
	Visceral fat (>0.58)	80.00 (32/40)	50.43* (59/117)	57.96* (91/157)	35.56* (32/90)	88.06 (59/67)
	SubQ fat (>0.39)	65.00 (26/40)	76.92 (90/117)	73.89 (116/157)	49.06 (26/53)	86.54 (90/104)
	Psoas muscle (>1.34)	70.00 (28/40)	84.62 (99/117)	80.89 (127/157)	60.87 (28/46)	89.19 (99/111)
Clinical predictor	BMI (≥25)	87.50 (35/40)	52.14* (61/117)	61.15* (96/157)	38.46 (35/91)	92.42 (61/66))
	Triglyceride	72.50 (29/40)	93.16 (109/117)	87.90 (138/157)	78.38 (29/37)	90.83 (109/120)
	HDL cholesterol	65.00 (26/40)	79.49 (93/117)	75.80 (119/157)	52.00 (26/50)	86.92 (93/107)
	Systolic pressure	72.50 (29/40)	62.39* (73/117)	64.97* (102/157)	39.73 (29/73)	86.90 (73/84)
	Diastolic pressure	45.00 (18/40)	79.49 (93/117)	70.70 (111/157)	42.86 (18/42)	80.87 (93/115)
	Fasting glucose (≥110)	62.50 (25/40)	88.89 (104/117)	82.17 (129/157)	65.79 (25/38)	87.39 (104/119)

BMI, body mass index; HDL, high-density lipoprotein; NPV, negative predictive value; PET/CT, positron emission tomography/computed tomography; PPV, positive predictive value; SubQ, subcutaneous.
*Significantly different to the psoas muscle ($P < 0.05$).
[a]Post hoc comparisons with Bonferroni correction using minimum required absolute difference test after Cochran's Q test.
[b]Post hoc comparison with Bonferroni correction after overall chi-squared test.
[c]Cut-off value is determined to maximize value of the Youden index for the ROC curve using Medcalc.

Table 5 Predictive performance of metabolic indicators for MetS measured in the validation group

Variable	AUROC[a]	Sensitivity[b]	Specificity[b]	Accuracy[b]	PPV[c]	NPV[c]
BMI (≥25)	0.789	80.95 (17/21)	56.15* (73/130)	59.60* (90/151)	22.97 (17/74)	94.81 (73/77)
Triglyceride	0.829	71.43 (15/21)	85.38 (111/130)	83.44 (126/151)	44.12 (15/34)	94.87 (111/117)
HDL cholesterol	0.765	57.14 (12/21)	85.38 (111/130)	81.46 (123/151)	38.71 (12/31)	92.50 (111/120)
Systolic pressure	0.767	76.19 (16/21)	75.38* (98/130)	75.50 (114/151)	33.33 (16/48)	95.15 (98/103)
Diastolic pressure	0.747	47.62 (10/21)	83.85 (109/130)	78.81 (119/151)	32.26 (10/31)	90.83 (109/120)
Fasting glucose (≥110)	0.695	61.90 (13/21)	76.15* (99/130)	74.17 (112/151)	29.55 (13/44)	92.52 (99/107)
Psoas muscle (>1.34[d])	0.709	47.62 (10/21)	92.31 (120/130)	86.09 (130/151)	50.00 (10/20)	91.60 (120/131)

AUROC, areas under the receiver operating characteristic; BMI, body mass index; NPV, negative predictive value; PPV, positive predictive value.
*Significantly different to the psoas muscle ($P < 0.05$).
[a]Pairwise Z-test with Bonferroni correction.
[b]Post hoc comparison with Bonferroni correction using minimum required absolute difference test after Cochran's Q test.
[c]Post hoc comparison with Bonferroni correction after overall chi-squared test.
[d]Cut-off value is determined in the experimental group to maximize value of the Youden index for the ROC curve using Medcalc.

Figure 2 Kaplan–Meier estimator plot of cumulative incidence for (A) metabolic syndrome and (B) risk determinants of metabolic syndrome in the two subgroups according to fluorodeoxyglucose uptake of psoas muscle (cut-off value of maximum standardized uptake value = 1.34). Significant differences were observed between the two subgroups (for all $P < 0.05$, except for hypertiglyceridemia).

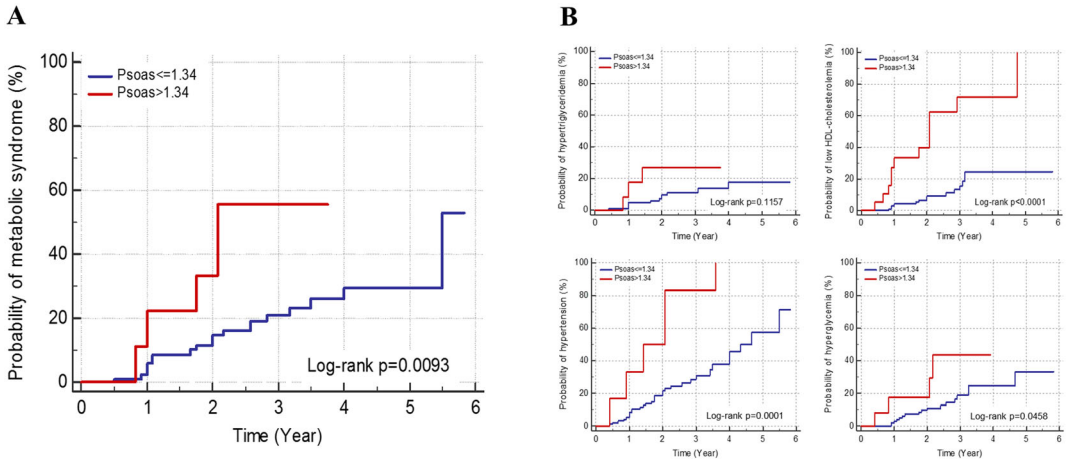

DOI: 10.1002/jcsm.12430

cholesterol (HR 7.15, $P < 0.0001$), hypertension (HR 5.59, $P = 0.0005$), and hyperglycaemia (HR 3.27, $P = 0.0392$) (Table S3).

Discussion

The ^{18}F-FDG uptake value in psoas muscle measured with ^{18}F-FDG PET/CT was positively correlated with clinical metabolic parameters and proved to be an independent risk factor for metabolic derangements including MetS. This was true even after adjustment for body weight, BMI, and other clinical determinants of MetS such as fasting glucose level. The ^{18}F-FDG uptake (SUV_{max}) in psoas muscle showed comparably valuable predictive diagnostic performances for existing MetS relative to the known clinical determinants thereof: BMI, triglyceride, HDL cholesterol, pressure, and fasting glucose. Specificity and accuracy were higher than those from some clinical parameters. Subjects with higher ^{18}F-FDG uptake ($SUV_{max} > 1.34$) in the psoas muscle showed a higher prevalence of existing MetS, and these patients also had significantly higher incidences of incipient MetS during clinical follow-up periods than did subjects with lower ^{18}F-FDG uptake ($SUV_{max} \leq 1.34$). Therefore, the ^{18}F-FDG uptake value in psoas muscle could be used as a valuable surrogate marker to predict metabolic derangement in clinical circumstances.

^{18}F-FDG is mainly taken up by glucose transporter type 4 (GLUT4) proteins in muscle. Glucose transport is a rate-limiting step for insulin-stimulated glucose utilization in skeletal muscle.[18,19] It is well known that GLUT4 is essential for insulin-mediated glucose transport in insulin-sensitive organs, including skeletal muscle, adipose tissue, and the heart.[20,21] The majority of insulin-dependent postprandial glucose uptake occurs in the skeletal muscle, and it is believed that IR on the part of GLUT4 in muscle plays a central role in the development of type 2 diabetes.[22,23] Increased insulin levels result in translocation of the GLUT4 protein from an intracellular pool to the plasma membrane,[24–26] and overexpression of GLUT4 might enhance the uptake of ^{18}F-FDG when injected in the fasting state. Our data suggested that the membrane fraction of GLUT4 expression in psoas muscle can be a surrogate marker of existing and incipient metabolic derangements. We are aware of three studies of ^{18}F-FDG uptake in skeletal muscle,[13,15,16] all of which contrasted with our findings. These reports showed that ^{18}F-FDG uptake of skeletal muscle was higher in lean healthy subjects than among those with diabetes.[13,15,16] All ^{18}F-FDG PET imaging in these studies was carried out on small numbers of insulin-stimulated subjects, using the glucose clamp test. ^{18}F-FDG PET imaging in our study was used in a routine clinical setting,[24,27] so was performed after 4–6 h of fasting. Excess additional insulin (glucose clamp test) in patients with diabetes or prediabetes subjects might cause saturation of overexpressed GLUT4, and the decreased amount of GLUT4 in the intracellular pool might cause insufficient translocation of GLUT4 in response to infused insulin. This might hinder the uptake of ^{18}F-FDG in hyperinsulinemic-euglycemic diabetes patients. To our knowledge, this is the first study that clinically applies ^{18}F-FDG PET measures of SMGU to evaluate metabolic disease. There has been no large-scale clinical study to determine the usefulness of of^{18}F-FDG uptake by skeletal muscle as a surrogate marker of existing or future metabolic derangement and systemic IR.

In our study, we used a validation group of subjects who underwent clinical follow-ups after ^{18}F-FDG PET imaging, to confirm the feasibility of predicting MetS. Both of the proportion of psoas $SUV_{max} \geq 1.34$ and the prevalence of MetS were significantly lower in this group than in the experimental group (proportion of $SUV_{max} \geq 1.34$: 23/158, 14.56% in Table S2 vs. 46/157, 29.30% in Table S1, $P = 0.0016$ by chi-squared test; for prevalence of MetS: 25/158, 15.82% vs. 40/157, 25.48%, Table 1, $P = 0.0342$). This might cause lower sensitivity and PPV in the validation group relative to those values calculated in the experimental group. However, the predictive performance for MetS of other clinical predictors showed similar results in the validation group.

This study has several limitations. First, we did not perform the glucose clamp test to identify the association between intramuscular IR and ^{18}F-FDG uptake in the psoas muscle. Second, dynamic PET imaging for kinetic analysis may have allowed accurate *in vivo* assessment of glucose transport and phosphorylation.[28,29] However, we used static PET imaging, which is more convenient for clinical application in a large-scale clinical study. Third, some studies have shown that GLUT expression may be increased on the surface of recruited macrophages and hypertrophied adipocytes and mediated by chronic low-grade inflammation in obese patients.[30,31] We did not do psoas muscle biopsies so did not check inflammatory cell infiltration in this muscle.

In conclusion, increased ^{18}F-FDG uptake in the psoas muscle successfully identified subjects with a significantly increased risk of incipient metabolic derangement and MetS, even though these individuals were not clinically classified with MetS at present.

Acknowledgements

This study was supported by the '2017 Young Faculty Forum' program, the research fund of Hanyang University (HY-201700000000081 and HY-201800000000233). The authors certify that they comply with the ethical guidelines for publishing in the Journal of Cachexia, Sarcopenia and Muscle: update 2017.[32]

Specific author contributions

Dae Won Jun contributed to the study design; Jun Choi did statistical analysis, Yun Young Choi analysed PET image; Ji Young Kim wrote the manuscript; Eunwoo Nam and Donghee Son did article review and statistical analysis.

Online supplementary material

Additional supporting information may be found online in the Supporting Information section at the end of the article.

Table S1 Comparison of metabolic parameters between psoas muscle groups in the experimental group

Table S2 Comparison of metabolic parameters between psoas muscle groups in the validation group

Table S3 Multiple Cox's proportional hazard regression analyses of psoas muscle groups for metabolic outcomes in the validation group

Conflicts of Interest

None of the authors have anything to declare.

References

1. Cheng S, Wiklund P. The effects of muscle mass and muscle quality on cardiometabolic risk in peripubertal girls: a longitudinal study from childhood to early adulthood. *Int J Obes (Lond)* 2018;**42**:648–654.
2. Kim TN, Park MS, Yang SJ, Yoo HJ, Kang HJ, Song W, et al. Body size phenotypes and low muscle mass: the Korean sarcopenic obesity study (KSOS). *J Clin Endocrinol Metab* 2013;**98**:811–817.
3. Yokoyama I, Inoue Y, Moritan T, Ohtomo K, Nagai R. Simple quantification of skeletal muscle glucose utilization by static 18F-FDG PET. *J Nucl Med* 2003;**44**:1592–1598.
4. Strauss LG, Conti PS. The applications of PET in clinical oncology. *J Nucl Med* 1991;**32**:623–648.
5. Hustinx R, Benard F, Alavi A. Whole-body FDG-PET imaging in the management of patients with cancer. *Semin Nucl Med* 2002;**32**:35–46.
6. Wahl RL, Jacene H, Kasamon Y, Lodge MA. From RECIST to PERCIST: evolving considerations for PET response criteria in solid tumors. *J Nucl Med* 2009;**50**:122S–150S.
7. Palatka K, Kacska S, Lovas S, Garai I, Varga J, Galuska L. The potential role of FDG PET-CT in the characterization of the activity of Crohn's disease, staging follow-up and prognosis estimation: a pilot study. *Scand J Gastroenterol* 2018;**53**:24–30.
8. Love C, Tomas MB, Tronco GG, Palestro CJ. FDG PET of infection and inflammation. *Radiographics* 2005;**25**:1357–1368.
9. Tawakol A, Migrino RQ, Bashian GG, Bedri S, Vermylen D, Cury RC, et al. In vivo 18F-fluorodeoxyglucose positron emission tomography imaging provides a noninvasive measure of carotid plaque inflammation in patients. *J Am Coll Cardiol* 2006;**48**:1818–1824.
10. Rudd JH, Warburton EA, Fryer TD, Jones HA, Clark JC, Antoun N, et al. Imaging atherosclerotic plaque inflammation with [18F]-fluorodeoxyglucose positron emission tomography. *Circulation* 2002;**105**:2708–2711.
11. Yoo HJ, Kim S, Hwang SY, Hong HC, Choi HY, Seo JA, et al. Vascular inflammation in metabolically abnormal but normal-weight and metabolically healthy obese individuals analyzed with ^{18}F-fluorodeoxyglucose positron emission tomography. *Am J Cardiol* 2015;**115**:523–528.
12. Chen W, Bural GG, Torigian DA, Rader DJ, Alavi A. Emerging role of FDG-PET/CT in assessing atherosclerosis in large arteries. *Eur J Nucl Med Mol Imaging* 2009;**36**:144–151.
13. Kelley DE, Mintun MA, Watkins SC, Simoneau JA, Jadali F, Fredrickson A, et al. The effect of non-insulin-dependent diabetes mellitus and obesity on glucose transport and phosphorylation in skeletal muscle. *J Clin Invest* 1996;**97**:2705–2713.
14. Kelley DE, Price JC, Cobelli C. Assessing skeletal muscle glucose metabolism with positron emission tomography. *IUBMB Life* 2001;**52**:279–284.
15. Yokoyama I, Yonekura K, Ohtake T, Kawamura H, Matsumoto A, Inoue Y, et al. Role of insulin resistance in heart and skeletal muscle F-18 fluorodeoxyglucose uptake in patients with non-insulin-dependent diabetes mellitus. *J Nucl Cardiol* 2000;**7**:242–248.
16. Goodpaster BH, Bertoldo A, Ng JM, Azuma K, Pencek RR, Kelley C, et al. Interactions among glucose delivery, transport, and phosphorylation that underlie skeletal muscle insulin resistance in obesity and type 2 diabetes: studies with dynamic PET imaging. *Diabetes* 2014;**63**:1058–1068.
17. Expert Panel on Detection E, Treatment of High Blood Cholesterol in A. Executive summary of the third report of the National Cholesterol Education Program (NCEP) expert panel on detection, evaluation, and treatment of high blood cholesterol in adults (Adult Treatment Panel III). *JAMA* 2001;**285**:2486–2497.
18. Katz A, Nyomba BL, Bogardus C. No accumulation of glucose in human skeletal muscle during euglycemic hyperinsulinemia. *Am J Physiol* 1988;**255**(Pt 1:E942–E945.
19. Ziel FH, Venkatesan N, Davidson MB. Glucose transport is rate limiting for skeletal muscle glucose metabolism in normal and STZ-induced diabetic rats. *Diabetes* 1988;**37**:885–890.
20. Kahn BB. Facilitative glucose transporters: regulatory mechanisms and dysregulation in diabetes. *J Clin Invest* 1992;**89**:1367–1374.
21. Mueckler M. Facilitative glucose transporters. *Eur J Biochem* 1994;**219**:713–725.
22. Cavallo-Perin P, Cassader M, Bozzo C, Bruno A, Nuccio P, Dall'Omo AM, et al. Mechanism of insulin resistance in human liver cirrhosis. Evidence of a combined receptor and postreceptor defect. *J Clin Invest* 1985;**75**:1659–1665.
23. Rizza RA, Mandarino LJ, Gerich JE. Mechanism and significance of insulin resistance in non-insulin-dependent diabetes mellitus. *Diabetes* 1981;**30**:990–995.
24. Cheung JY, Conover C, Regen DM, Whitfield CF, Morgan HE. Effect of insulin on kinetics of sugar transport in heart muscle. *Am J Physiol* 1978;**234**:E70–E78.
25. Sun D, Nguyen N, DeGrado TR, Schwaiger M, Brosius FC 3rd. Ischemia induces translocation of the insulin-responsive glucose transporter GLUT4 to the plasma membrane of cardiac myocytes. *Circulation* 1994;**89**:793–798.
26. Lindholm P, Minn H, Leskinen-Kallio S, Bergman J, Ruotsalainen U, Joensuu H. Influence of the blood glucose concentration on FDG uptake in cancer—a PET study. *J Nucl Med* 1993;**34**:1–6.
27. Boellaard R, Delgado-Bolton R, Oyen WJ, Giammarile F, Tatsch K, Eschner W, et al. FDG PET/CT: EANM procedure guidelines for tumour imaging: version 2.0. *Eur J Nucl Med Mol Imaging* 2015;**42**:328–354.
28. Fowler JS, Wolf AP. 2-Deoxy-2-[18F]fluoro-D-glucose for metabolic studies: current

status. *Int J Rad Appl Instrum A* 1986;**37**:663–668.
29. Huang SC, Williams BA, Barrio JR, Krivokapich J, Nissenson C, Hoffman EJ, et al. Measurement of glucose and 2-deoxy-2-[18F]fluoro-D-glucose transport and phosphorylation rates in myocardium using dual-tracer kinetic experiments. *FEBS Lett* 1987;**216**:128–132.
30. Freemerman AJ, Johnson AR, Sacks GN, Milner JJ, Kirk EL, Troester MA, et al. Metabolic reprogramming of macrophages: glucose transporter 1 (GLUT1)-mediated glucose metabolism drives a proinflammatory phenotype. *J Biol Chem* 2014;**289**: 7884–7896.
31. Shepherd PR, Kahn BB. Glucose transporters and insulin action—implications for insulin resistance and diabetes mellitus. *N Engl J Med* 1999;**341**:248–257.
32. von Haehling S, Morley JE, Coats AJS, Anker SD. Ethical guidelines for publishing in the Journal of Cachexia, Sarcopenia and Muscle: update 2017. *J Cachexia Sarcopenia Muscle* 2017;**8**:1081–1083.